

# A nano-sized blending system comprising identical triblock copolymers with different hydrophobicity for fabrication of an anticancer drug nanovehicle with high stability and solubilizing capacity

This article was published in the following Dove Press journal:  
*International Journal of Nanomedicine*

Ngoc Ha Hoang<sup>1,\*</sup>  
Tae-hoon Sim<sup>1,\*</sup>  
Chaemin Lim<sup>1</sup>  
Thi Ngoc Le<sup>1</sup>  
Sang Myung Han<sup>1</sup>  
Eun Seong Lee<sup>2</sup>  
Yu Seok Youn<sup>3</sup>  
Kyung Taek Oh<sup>1</sup>

<sup>1</sup>College of Pharmacy, Chung-Ang University, Dongjak-gu, Seoul 06974, Korea; <sup>2</sup>Department of Biotechnology, The Catholic University of Korea, Bucheon, Gyeonggi-do 14662, Korea; <sup>3</sup>School of Pharmacy, Sungkyunkwan University, Suwon City 16419, Korea

\*These authors contributed equally to this work

**Background:** A very common and simple method (known as the blending method) to formulate drug delivery systems with required properties is to physically mix amphiphilic block copolymers with different hydrophobicity. In addition to its simplicity, this blending strategy could help avoid the time and effort involved in the synthesis of block copolymers with the desired structure required for specific drug formulations.

**Purpose:** We used the blending strategy to design a system that could overcome the problem of high hydrophobicity and be a good candidate for drug product development using PEG-PLA-PEG triblock copolymers.

**Methods:** Two types of PEG-PLA-PEG triblock copolymers with similar (long) PLA molecular weights (MWs) and different PEG MWs were synthesized. The micellar formulations were prepared by blending the two block copolymers in various ratios. The size and stability of the blending systems were subsequently investigated to optimize the formulations for further studies. The loading properties of doxorubicin or paclitaxel into the optimized blending system were compared to that in mono systems (systems composed of only a single type of triblock copolymer). In vitro and in vivo anti-cancer effects of the preparations were evaluated to assess the use of the blending system as an optimal nanomedicine platform for insoluble anticancer agents.

**Results:** The blending system (B20 system) with an optimized ratio of the triblock copolymers overcame the drawbacks of mono systems. Drug uptake from the drug-loaded B20 system and its anticancer effects against KB cells were superior compared to those of free drugs (doxorubicin hydrochloride and free paclitaxel). In particular, doxorubicin-loaded B20 resulted in extensive doxorubicin accumulation in tumor tissues and significantly higher in vivo anti-cancer effects compared to free doxorubicin.

**Conclusion:** The blending system reported here could be a potential nanoplatform for drug delivery due to its simplicity and efficiency for pharmaceutical application.

**Keywords:** blending system, block copolymer, triblock copolymer, drug delivery, nanomedicine, cancer

## Introduction

Nanosized micelles with core-shell structures using amphiphilic block copolymers have been widely developed for successful drug delivery.<sup>1-5</sup> It is well known that the hydrophilicity-hydrophobicity ratio of amphiphilic block copolymers has major effects on the properties of drug delivery systems.<sup>6,7</sup> Micelles prepared using amphiphilic block copolymers with high hydrophobicity showed a high loading

Correspondence: Kyung Taek Oh  
College of Pharmacy, Chung-Ang  
University, 84 Heukseok-ro, Dongjak-gu,  
Seoul 06974, Korea  
Tel +82 2 820 5617  
Email kyungoh@cau.ac.kr

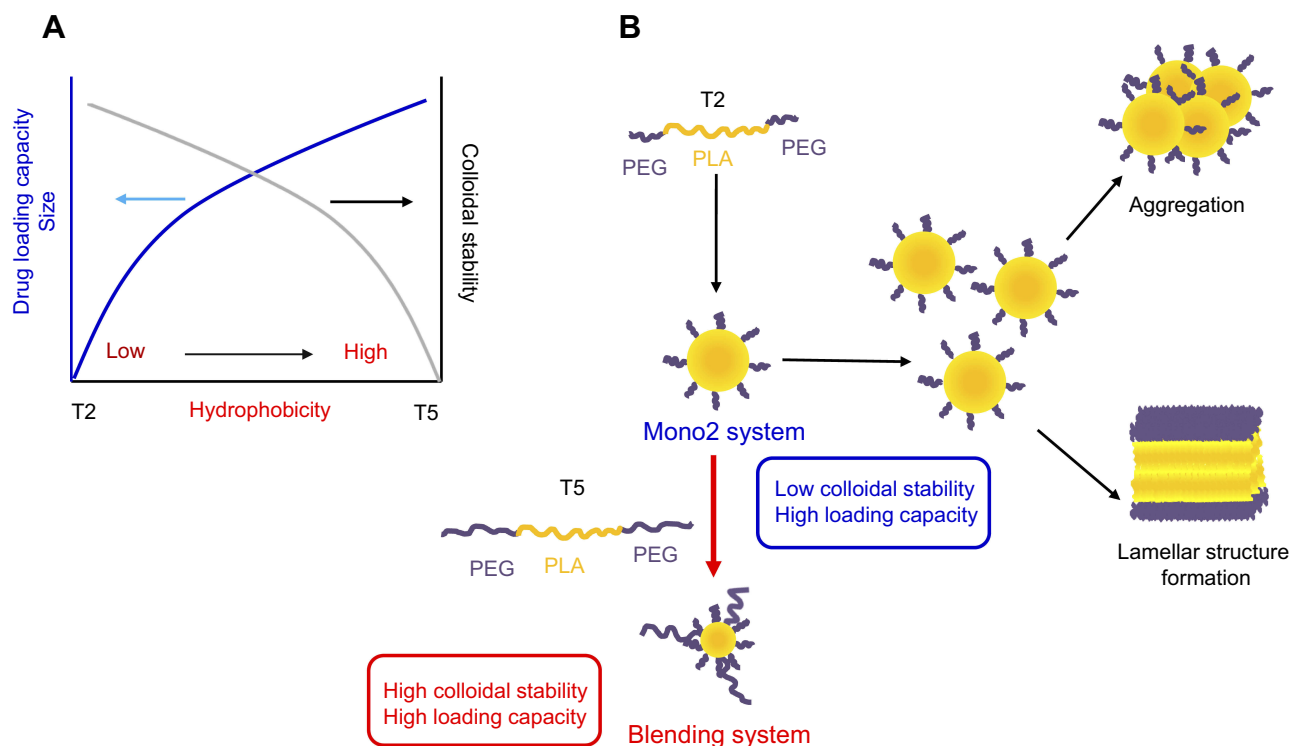


**Figure 1** Schematic concept of the blending system using amphiphilic block copolymers. **(A)** Effects of hydrophobic ratio on physicochemical properties of micelles. **(B)** Formation of optimized micellar system by blending different triblock copolymers. T2, PEG-PLA-PEG triblock copolymer (2 K-10 K-2 K); T5, PEG-PLA-PEG triblock copolymer (5 K-10 K-5 K).

**Abbreviation:** PEG-PLA-PEG, poly(ethylene glycol)-poly(lactic acid)-poly(ethylene glycol).

capacity but very limited colloidal stability (Figure 1A). The low colloidal stability of micelles might explain why most clinically approved nanomicellar drug products use amphiphilic block copolymers with relatively high hydrophilicity.<sup>8</sup> This would lead to the utilization of very large amounts of amphiphilic block polymer in the formulations to compensate for the poor drug-loading capacity, potentially resulting in toxicity in patients. These types of micelles also have a high critical micelle concentration (CMC) and low kinetic stability in drug incorporation, potentially leading to burst releases of drugs in the bloodstream, causing insufficient accumulation of drugs at target tissues. Therefore, the design of micellar drug formulations with high colloidal and kinetic stability as well as high loading capacity is critical in developing drug products based on amphiphilic block copolymers.

A very common and simple method (known as the blending method) to formulate drug delivery systems with required properties is to physically mix amphiphilic block copolymers with different hydrophobicity. In addition to its simplicity, this blending strategy could help avoid the time and effort involved in the synthesis of block copolymers with the desired structure required for specific drug formulations.

Previously, blending systems combining Pluronics<sup>®</sup> with different hydrophilicity have been studied.<sup>9–12</sup> In particular, combination micelles with Pluronics<sup>®</sup> L61 and F127 (SP1049C, currently developed by Supratek Pharma Inc, IncDorval, QC, Canada.) have been in Phase III clinical trials for the treatment of doxorubicin-resistant cancers.<sup>11,13</sup> However, the application of Pluronics<sup>®</sup> in parenteral pharmaceutical products is very limited due to their nonbiodegradability and consequent potential toxicity, especially in long-term utilization.<sup>12,14,15</sup> Poly(ethylene glycol)-poly(lactic acid)-poly(ethylene glycol) (PEG-PLA-PEG) appears to be the ideal alternative to Pluronics<sup>®</sup> in the development of drug delivery systems due to its biodegradable and biocompatible nature, and its structural similarity to Pluronics<sup>®</sup>.<sup>7,16,17</sup> Previously, our group reported a simple method to synthesize PEG-PLA-PEG and its potential in drug formulations to treat metastatic cancer.<sup>17</sup> It was also demonstrated that the properties of micelles based on PEG-PLA-PEG with different structures are largely dependent on the hydrophilicity/hydrophobicity ratio.<sup>7</sup> However, it was challenging to achieve ideal properties for drug delivery using single-type micelles of PEG-PLA-PEG, as with other copolymers (Figure 1A). PEG-PLA-PEG with high PLA

content has good drug-loading capacity but very low colloidal stability, making it quite challenging to use in drug product development. To achieve high drug-loading capacity and high colloidal stability, blending different polymers would be more practical than modulating intramolecular properties such as the hydrophilicity/hydrophobicity ratio depending on the polymer used.

In the present study, we used the blending strategy to design a system that could overcome the above problem of high hydrophobicity and be a good candidate for drug product development. Two types of PEG-PLA-PEG triblock copolymers with similar (long) PLA molecular weights (MWs) and different PEG MWs were synthesized. The micellar formulations were prepared by blending the two block copolymers in various ratios. The size and stability of the blending systems were subsequently investigated to optimize the formulations for further studies. The loading properties of doxorubicin (DOX) or paclitaxel (PTX) into the optimized blending system were compared to that in monosystems (systems based on a single type of PEG-PLA-PEG). In vitro and in vivo anticancer effects of the preparations were evaluated to assess the use of the blending system as an optimal nanomedicine platform for insoluble anticancer agents.

## Materials and methods

### Materials

PEG (MW 2 kDa, abbreviated as 2 K), methoxy poly(ethylene glycol) (mPEG; MW 2 K), L-lactide ((3S)-cis-3,6-dimethyl-1,4-dioxane-2,5-dione), N,N-dicyclohexylcarbodiimide (DCC), stannous octoate (tin(II)-2-ethylhexanoate, Sn(Oct)<sub>2</sub>), 4-dimethylaminopyridine (DMAP), dimethylsulfoxide (DMSO), succinic anhydride, pyridine, and triethylamine (TEA) were purchased from Sigma-Aldrich (St. Louis, MO, USA). Tetrahydrofuran (THF), toluene, acetone, and dichloromethane (DCM) were purchased from Honeywell Burdick & Jackson<sup>®</sup> (Muskegon, MI, USA). Doxorubicin (DOX)•HCl was purchased from Boryung Co. (Jongro-gu, Seoul, Korea). Paclitaxel was obtained from Samyang Co. (Seongnam-si, Gyeonggi-do, Korea). Diethyl ether and hexane were purchased from Samchun Chemical (Gangnam-gu, Seoul, Korea). Fluorescein-5-isothiocyanate (FITC-5-isothiocyanate) was purchased from Thermo Fisher Scientific (Waltham, MA, USA). KB cells were obtained from the Korean Cell Line Bank (Jongno-gu, Seoul, Korea). RPMI 1640 medium, Dulbecco's Phosphate-Buffered Saline (DPBS), penicillin–streptomycin solution, trypsin–EDTA solution, and FBS were purchased from

Welgene (Gyeongsan-si, Gyeongsangbuk-do, Korea). The Cell Counting Kit-8 (CCK-8) was purchased from Dojindo Molecular Technologies, Inc. (Rockville, MD, USA). The Pierce™ BCA Protein Assay Kit was obtained from Thermo Fisher Scientific.

## Methods

### Triblock copolymer synthesis

PEG-PLA-PEG triblock copolymers with or without functional groups were synthesized using procedures described previously (Figure S1 and Table S1).<sup>17–19</sup> FITC was conjugated to PEG-PLA-PEG triblock copolymer 2 K-10 K-2 K via the interaction of FITC-5-isothiocyanate with free –OH groups on functional PEG-PLA-PEG triblock copolymers. Briefly, functional PEG-PLA-PEG and FITC-5-isothiocyanate (molar ratio 1:3) were added to a round-bottom flask and 30 mL of DMSO was then added. The reaction was allowed to proceed for 24 hrs at room temperature. Free FITC-5-isothiocyanate in the reactant mixture was then removed via dialysis against 1 L of water for 24 hrs. FITC-PEG-PLA-PEG powder was obtained via lyophilization. Micelles used for in vivo imaging contained 10 wt% of FITC-PEG-PLA-PEG.

### Preparation of self-assembled polymeric micelles

Polymeric micelles were prepared using a dialysis method. The triblock copolymer or a mixture of different triblock copolymers (10 mg) was dissolved in 3 mL of DMSO. The triblock copolymer solution in DMSO was then transferred to dialysis membrane bags (MWCO 3.5 KDa, Spectra, Repligen, Waltham, MA, USA) and dialyzed against PBS at pH 7.4 for 24 hrs.

### CMC determination

Fluorescence measurements to evaluate the CMC was performed using a Scinco FS-2 fluorescence spectrometer (Gangnam-gu) equipped with polarizers for excitation and emission. Pyrene was used as the fluorescent probe. The sample solutions were prepared by adding pyrene solution in acetone to empty amber vials. After evaporation, micelle solutions with different concentrations of triblock copolymers were added to the vials resulting in a final pyrene concentration of  $6 \times 10^{-7}$  M. These samples were stirred overnight at room temperature. Excitation spectra of pyrene in the samples were recorded at  $\lambda_{em}=374$  nm at room temperature. CMC was estimated by plotting the ratio of  $I_{336}$  (fluorescence

intensity at 336 nm) to  $I_{334}$  (fluorescent intensity at 334 nm) of the excitation spectra against logarithms of the copolymer concentrations. The CMC was defined as the crossover point of low copolymer concentrations on the plot.<sup>20,21</sup>

## Particle size measurement

The particle sizes (effective hydrodynamic diameters) of micelles were measured via photon correlation spectroscopy using Zetasizer Nano-ZS (Malvern Instruments, Malvern, UK) equipped with the multiangle sizing option (BI-MAS). The measurements were performed in a thermostatic cell at a scattering angle of 90°. Software provided by the manufacturer was used to calculate effective hydrodynamic diameter values.

## Morphology

Diluted micelle dispersions prepared using PBS were deposited onto a slide glass and dried under vacuum. Field emission scanning electron microscopy (FE-SEM) examinations were performed after platinum (Pt) coating the samples. The morphology of the polymeric micelle was examined using FE-SEM (Sigma, Carl Zeiss, Germany).

## Preparation and characterization of drug-loaded micelles

For the preparation of DOX-loaded micelles, DOX•HCl was blended with TEA at a 1:2 molar ratio in DMSO overnight to generate doxorubicin base (DOX). Five milligrams of DOX•HCl was mixed with 10 mg of triblock copolymer in DMSO and dialyzed (Molecular weight cutoff [MWCO] 3.5 kDa, Spectrum) against PBS at pH 7.4 for 24 hrs. To prepare PTX-loaded micelles, 1 mg of PTX was mixed with 10 mL of triblock copolymer in DMSO and dialyzed against PBS at pH 7.4 for 24 hrs. The solutions were then centrifuged at 5,000 rpm for 5 mins to precipitate nonloaded drug. Supernatants containing drug-loaded micelles were then collected. The concentrations of DOX in the micelles were determined using a UV-Vis spectrometer (GENESYS 10 UV, Thermo Fisher Scientific) at a wavelength of 481 nm. The concentrations of PTX in the micelles were determined using a high-performance liquid chromatography system (Agilent 1,200 series, Agilent Technologies, Santa Clara, CA, USA) equipped with an auto-injector, high-pressure gradient pump, and UV-Vis detector at a wavelength of 230 nm.

Drug loading capacity was calculated using the following equation:

$$\text{Drug loading capacity (wt \%)} \\ = (\text{weight of loaded drug in micelles} / \text{weight of polymer and drug}) \times 100$$

## Cellular uptake

### DOX uptake via flow cytometry

The cellular uptake of DOX•HCl and DOX-loaded micelles was determined using flow cytometry. KB cells were maintained in RPMI 1640 supplemented with 10% FBS in a humidified incubator at 37°C in 5% CO<sub>2</sub>. KB cells were seeded into 6-well plates (2×10<sup>5</sup> cells/well in 3 mL media) and incubated at 37 °C in 5% CO<sub>2</sub> for 24 hrs. The media were then removed and DOX•HCl solutions or DOX-loaded micelle solutions at a concentration of 5 µg/mL were added. The plate was incubated at 37°C in 5% CO<sub>2</sub> for 3 hrs. The cells were then washed three times with cold PBS and harvested with scrapers. DOX uptake from DOX•HCl solutions or DOX-loaded micelle was determined subsequently using a BD FACS Calibur flow cytometer with Cell Quest Pro software (BD Biosciences, San Diego, CA, USA).

### DOX uptake via confocal microscopy

The in vitro uptake of DOX into KB cells was also confirmed using confocal microscopy. KB cells were grown in 6-well plates (1.5×10<sup>5</sup> cells per well) containing a cover glass in each well. After 24 hrs, media were replaced with solutions of DOX•HCl or DOX-loaded blending systems at a DOX concentration of 1 µg/mL in media. Cells fed with only media were included as controls. After 3 hrs of incubation, the media were removed and the cells on cover glasses were washed three times with cold DPBS. They were then fixed using paraformaldehyde solution (4%) in water for 15 mins. They were subsequently washed again three times with cold DPBS. Next, cell nuclei were stained with DAPI (Thermo Fisher Scientific) using the protocol provided by the manufacturer. Finally, cover glasses were mounted on glass slides using Permount<sup>®</sup> mounting medium (Thermo Fisher Scientific). DOX uptake was observed using an LSM800 Confocal Laser Scanning Microscope (Carl Zeiss, Oberkochen, Germany).

### PTX uptake

KB cells were seeded into 6-well plates (2×10<sup>5</sup> cells/well in 3 mL media) and incubated at 37°C in 5% CO<sub>2</sub> for 24 hrs. The



media were then removed and 1  $\mu\text{g}/\text{mL}$  of PTX solution or PTX-loaded micelle solutions was added. The plates were incubated at  $37^\circ\text{C}$  in 5%  $\text{CO}_2$  for 6 hrs. They were then washed three times with cold PBS and harvested with scrapers and centrifuged at 5,000 rpm for 5 mins. After the centrifugation, the supernatants were removed, and 1 mL of 0.1% Triton X-100 in PBS was added to lyse the cells. The lysates were then centrifuged at 15,000 rpm for 15 mins and supernatants were collected. The protein concentrations of the supernatants were subsequently determined using a BCA kit. The samples were freeze-dried, and PTX concentrations were determined using a high-performance liquid chromatography system (Agilent 1,200 series, Agilent Technologies) equipped with an auto-injector, high-pressure gradient pump, and UV-Vis detector at a wavelength of 230 nm. The cellular uptake of PTX from free PTX solutions and PTX-loaded micelle solutions were compared by calculating the ratio of PTX to total cellular protein (PTX/protein).

## In vitro anticancer effect

The cytotoxicity of free drugs (DOX•HCl and PTX) or drug-loaded micelles against KB cells was assessed using a CCK-8 viability assay. The cells were seeded in 96-well plates at 5,000 cells per well in 100  $\mu\text{L}$  of RPMI 1640 supplemented with 5% FBS, 1% penicillin–streptomycin, and incubated at  $37^\circ\text{C}$  in 5%  $\text{CO}_2$  for 24 hrs. Next, the media were removed, and the cells were washed with DPBS. One hundred microliters of drug solutions or drug-loaded micelle solutions was added at different concentrations and the cells were incubated at  $37^\circ\text{C}$  in 5%  $\text{CO}_2$  for 48 hrs. The viability of KB cells was determined using CCK assays. Fresh medium containing CCK solution (10 vol%) was added to each well. The plates were incubated for an additional 3 hrs. The absorbance in each well was then read on a Flexstation 3 microplate reader (Molecular Devices, Sunnyvale, CA, USA) at a wavelength of 450 nm. The viability of cells treated with micelles was compared with that of untreated cells.  $\text{IC}_{50}$  values of free drugs and drug-loaded micelles were calculated using GraphPad Prism 5 software (San Diego, CA, USA).

## In vivo studies

### Animal care

Animal care and all animal experiments were performed in accordance with the National Institute of Health guidelines “Principles of laboratory animal care” and the “Animal Protection Law in Republic of Korea” and were approved by the Institutional Animal Care and Use Committee (IACUC) of

Chung-Ang University, Seoul, Republic of Korea. Tumor xenografts were established by subcutaneously injecting  $1 \times 10^6$  of KB cells suspended in 0.1 mL of DPBS into the right flanks of BALB/c nude mice (Orient Bio Inc., Seoul, Korea). Tumor volume was calculated using the following equation: tumor volume = length  $\times$  (width)<sup>2</sup>/2.<sup>22–25</sup> Studies of micelle biodistribution and anticancer effects were initiated when the tumor volume reached approximately 100  $\text{mm}^3$ .

### Biodistribution of drug-loaded micelles

PEG-PLA-PEG micelle solutions (1 mg/mL) containing 10 wt% of FITC-PEG-PLA-PEG were injected into the tail vein of mice-bearing tumors. The biodistribution of micelles at different time points after injection were monitored using a fluorescence in vivo imaging system (FOBI system, Neo Science, Suwon, Korea) with the channel set to detect the green color of FITC. Twenty four hours after injection, the tumor and other main organs were then isolated to check the accumulation of micelles. The in vivo and ex vivo fluorescence levels were determined using NEOimage software (Neo Science, Suwon, Korea).

### In vivo anticancer efficacy and toxicity

BALB/c nude mice-bearing tumors were randomly divided into three groups, and 0.2 mL of DOX•HCl or DOX-loaded micelle solutions in water was injected into their tail veins at a dose of 2 mg/kg at study initiation. Mice in the control group received intravenous injection of PBS (0.2 mL) into the tail veins. Change in tumor sizes and body weights of the mice was monitored every 3 days for 27 days. At the end of the study, mice were euthanized, and the tumors were collected for size comparisons. One-way ANOVA was used for statistical comparison, and Dunnett’s test was used as the post hoc test.

## Results and discussion

### Blending system optimization

In a previous report, micelles prepared using PEG-PLA-PEG (2 K-10 K-2 K) had high drug-loading capacity but showed significantly limited colloidal stability (Table 1).<sup>18</sup> The low colloidal stability may lead to aggregation of micelles, resulting in potential problems in biodistribution. Because large particles have been reported to be more susceptible to the mononuclear phagocyte system, they may be unable to enter small capillaries and other sites which are accessible to smaller particles.<sup>6,26</sup>

To improve colloidal stability, a small amount of PEG-PLA-PEG with longer PEG was incorporated because colloidal stability strongly depends on the length and density of the

hydrophilic layer on the micelle surfaces (Figure 1B).<sup>6,27</sup> In the present study, PEG-PLA-PEG (2 K-10 K-2 K, T2)<sup>18</sup> was simply mixed with PEG-PLA-PEG (5 K-10 K-5 K, T5), which has increased hydrophilic PEG density. Blending systems with various ratios were prepared and characterized to evaluate particle size and stability (Table 1 and Figure 2A). Mono 5 micelles solely composed of T5 had a particle size of approximately 125 nm and extremely high colloidal stability. Previously, we showed that Mono 2 had a very big particle size (approximately 417 nm) and extremely low colloidal stability.<sup>7</sup> The size of the blending system decreased as the amount of T5 was decreased. Mono 2 and the B10 blending system which had 10 wt% of T5 had very low colloidal stability with the size reaching approximately 1,000 nm after 1 week storage at room temperature, because a high hydrophobic–hydrophilic ratio could have led to the reduction of CMC resulting in poor thermodynamic stability.<sup>6</sup> As the T5 amount increased to 20 wt% or more, the blending system micelles had a particle size of approximately 150 nm with high colloidal stability. Interestingly, the micelle sizes did not decrease anymore at a higher ratio of T5, indicating that 20 wt% of T5 was sufficient to generate repulsive forces among the micelles to prevent aggregation. The polydispersity index of the prepared micelles indicating the stability of the nanoparticles also revealed effects of additional T5 on the stability of the micelles (Tables 1 and 2). Considering the particle size and colloidal stability, the B20 system was selected as the most suitable nanoplatform for further studies.

To confirm the stability of the B20 system, the CMC of the system was compared to those of the mono 2 and mono 5 systems. In a previous study, we revealed that Mono 2 had very low CMC, approximately 6.5 µg/mL, due to its high hydrophobicity.<sup>7</sup> Interestingly, the B20 system had a very low CMC value, <8 µg/mL (Table 2), indicating its high thermodynamic stability. This indicated that relatively low amounts of triblock copolymers with a

high hydrophilicity–hydrophobicity ratio would not significantly affect the assembly of the block copolymers into micelles. As discussed,<sup>6</sup> a low CMC value determines the thermodynamic stability of micelles and their integrity when diluted in high volumes in the bloodstream. Therefore, the B20 system with a persistent low CMC was found to be a system with high potential for clinical translation.

## Morphologies of micelles

To clarify the relationship between stability and morphology of the micelles, the mono 2, B20, and mono 5 systems were observed immediately after preparation and 1 week after storage at room temperature using FE-SEM (Figure 2B and C). The morphology of the mono 2 system micelles changed from a spherical shape to a rod-like shape during storage, while the B20 and mono 5 micelles retained their spherical shape. Interestingly, aggregation of the mono 2 micelles was observed immediately after preparation (Figure 2B). This demonstrated that the micelles prepared using triblock copolymers with a high hydrophobicity–hydrophilicity ratio may possess a greater tendency to aggregate and may lead to potential sphere-to-rod transition. This suggested that mono 2 could form a kinetical spherical micelle by diafiltration technique and thermodynamically formed a cylindrical aggregation due to lack of the spherical hindrance by relatively shorter PEG and greater hydrophobic interactions with longer PLA. Because T5 block copolymers with longer hydrophilic segments were added, the micellar system retained spherical shapes due to the sterically stabilizing effect of long PEG chains.<sup>9,28</sup> In other words, the morphologies of the micellar systems could be controlled by varying the length of hydrophobic PLA and hydrophilic PEG segments.

**Table 1** Characteristics of different blending systems depending on the composition of T5 and T2 polymers

System	PEG-PLA-PEG (wt%)		Size (nm) <sup>a</sup>	PDI	Stability
	5K-10K-5K (T5)	2K-10K-2K (T2)			
Mono 2	0	100	NA	NA	NA
B10	10	90	297±11.2	0.23±0.06	Unstable <sup>b</sup>
B20	20	80	150±4.4	0.14±0.01	Stable <sup>c</sup>
B30	30	70	144±5.1	0.13±0.03	Stable <sup>c</sup>
B40	40	60	149±1.6	0.14±0.02	Stable <sup>c</sup>
Mono 5	100	0	125±3.5	0.17±0.04	Stable <sup>c</sup>

**Notes:** <sup>a</sup>Determined using dynamic light scattering (DLS) at 25°C. Means ± SD, n=3. <sup>b</sup>Aggregation occurred within 1 day. <sup>c</sup>Stable for at least 1 week. NA indicates the data is not available see Hoang et al for more information.<sup>7</sup>

**Abbreviations:** PEG-PLA-PEG, poly(ethylene glycol)-poly(lactic acid)-poly(ethylene glycol); PDI, polydispersity index.

## Drug-loading properties of the micellar systems

To evaluate drug-loading properties of the blending system, DOX and PTX were used as typical poorly water-soluble drugs and were loaded into the mono 2,<sup>7</sup> B20, and mono 5 systems. Like previously proved with DOX-loaded Mono 2,<sup>7</sup> the drug-loaded micelles showed increased particle sizes in all the micellar systems (Table 2), due to drug loading into the micellar cores.<sup>19,29</sup> Interestingly, PTX affected the micelle size more than DOX, although the PTX loading capacities were

lower than the DOX-loading capacities. This was probably due to the lower compatibility between PTX and PLA compared to that between DOX and PLA in the micelle core.

The mono 2<sup>7</sup> and mono 5 systems had the highest and lowest drug-loading capacities, respectively. Although the DOX- and PTX-loading capacities of B20 were lower than those of the mono 2 system ( $13.57 \pm 0.64$  and  $6.99 \pm 1.55\%$  compared to  $17.54 \pm 0.61^7$  and  $7.16 \pm 0.33\%$ , respectively), the differences were not significant. Remarkably, loading capacities of the B20 system were approximately three times higher than

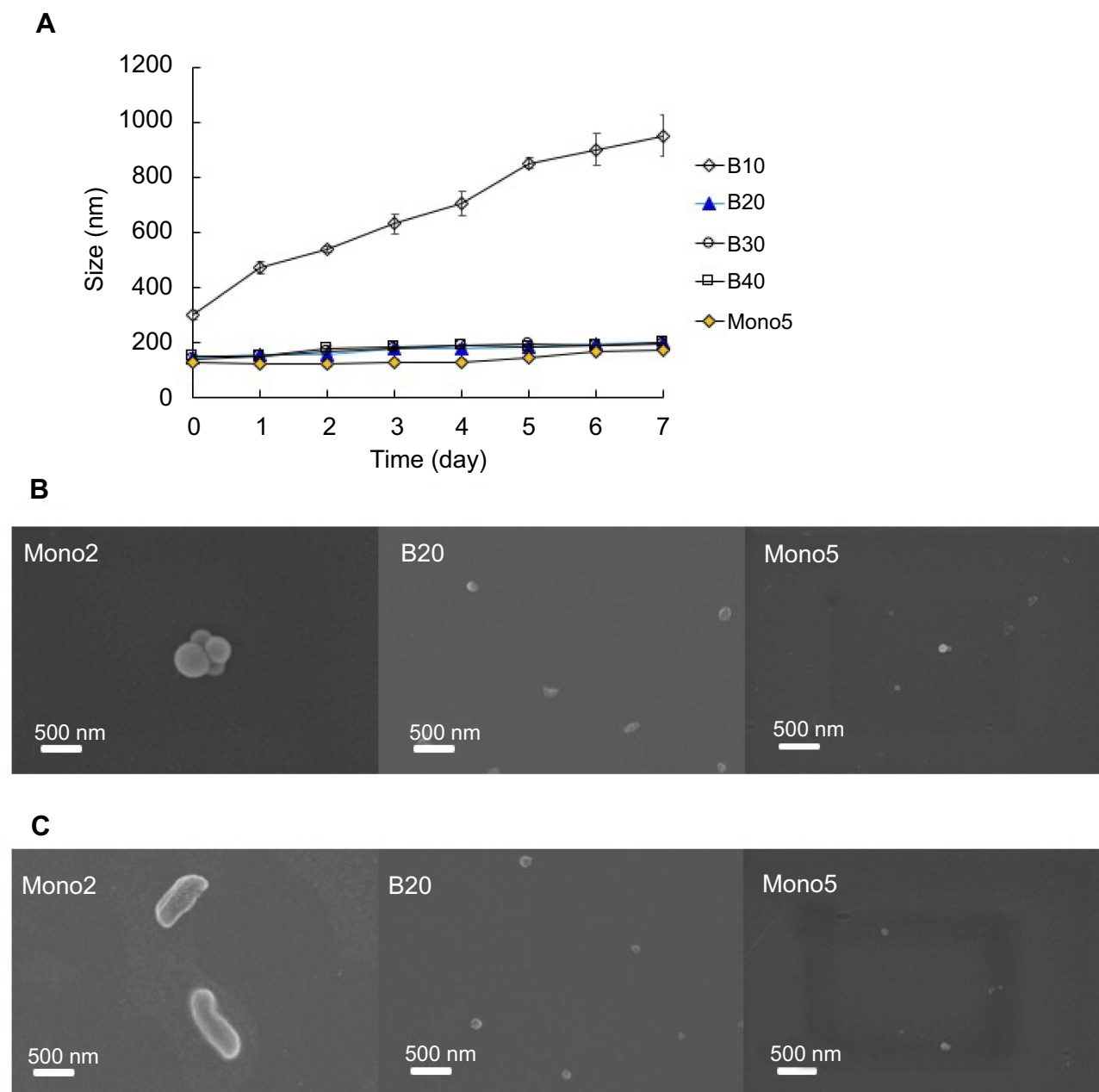


**Figure 2** Colloidal stability of the micellar systems. **(A)** The change in particle sizes of different systems was monitored daily (within 1 week after preparation). **(B and C)** The morphologies of different systems observed **(B)** immediately after preparation and **(C)** after 7-day storage at room temperature. For information on Mono 2 colloidal stability see Hoang et al.<sup>7</sup>

**Table 2** CMC and characterization of drug-loaded micellar systems

Systems	CMC ( $\mu\text{g/mL}$ ) <sup>a</sup>	Drug-loading properties of micelles <sup>a</sup>					
		DOX			PTX		
		LC (%)	Size (nm)	PDI	LC <sup>b</sup> (%)	Size (nm)	PDI
<b>Mono 2</b>	NA	NA	NA	NA	7.19 $\pm$ 0.33	570 $\pm$ 35.2	0.33 $\pm$ 0.01
<b>B20</b>	6.42 $\pm$ 0.893	13.57 $\pm$ 0.64	162 $\pm$ 9.7	0.17 $\pm$ 0.04	6.99 $\pm$ 1.55	175 $\pm$ 5.1	0.19 $\pm$ 0.05
<b>Mono 5</b>	17.91 $\pm$ 1.127	4.31 $\pm$ 0.54	150 $\pm$ 3.2	0.18 $\pm$ 0.01	2.21 $\pm$ 0.97	155 $\pm$ 6.8	0.21 $\pm$ 0.02

Notes: <sup>a</sup>Mean  $\pm$  SD, n=3. NA indicates the data is not available see Hoang et al for more information.<sup>7</sup>

Abbreviations: PEG-PLA-PEG, poly(ethylene glycol)-poly(lactic acid)-poly(ethylene glycol); PDI, polydispersity index; DOX, doxorubicin; PTX, paclitaxel; CMC, critical micelle concentration; LC, loading capacity.

those of the mono 5 system. Higher drug-loading capacities of the mono 2 and B20 systems compared to that of the mono 5 system were probably due to the higher ratio of hydrophobic blocks, which formed the micelle core serving as cargo space for drugs. Drug-loading capacity of micelles depends on several factors such as the nature of the solute, the property of core-forming blocks, and the length of core blocks.<sup>6,30,31</sup>

These results suggested that the blending of block copolymers could be an efficient strategy to increase the loading capacity of micelles for poorly water-soluble drugs. The improved drug-loading capacity and high stability demonstrated that the B20 system featured the strengths of both the triblock polymers (Tables 1 and 2). Therefore, the B20 system, with its high thermodynamic and colloidal stability and high drug-loading capacities, would be a promising nanoplatform for future studies.

## In vitro studies

DOX-loaded and PTX-loaded B20 systems (DOX/B20 and PTX/B20) were then used in vitro studies. First, the uptake of DOX/B20 and PTX/B20 into KB cancer cells was evaluated and compared to that of free DOX and PTX, respectively. Interestingly, the uptake of DOX/B20 into KB cells was 3–4 times higher than that of free DOX (Figure 3A and B). The mean fluorescence intensity of DOX/B20 was 31.65, which was a remarkable enhancement in cellular uptake compared to that of DOX (the mean FI: 11.19). PTX/B20 also resulted in 2.83-fold higher PTX amount compared to free PTX, which was a statistically significant difference ( $p < 0.05$ , Figure 3C). The cellular uptake of drug-loaded micelles via endocytosis<sup>26,32–34</sup> might be faster than simple diffusion, which is the main uptake mechanism of free drugs.<sup>34–36</sup> Further, drug-release profiles of DOX- and PTX-loaded micelles were compared as an underlying factor in the cell viability study (Figure S2). Consistent with the colloidal stability of the micellar systems (Figure 2), B20 and mono 5 showed higher drug release than the mono 2 system,<sup>7</sup>

probably because the mono 2 system possessed a highly hydrophobic micelle core and high compatibility with hydrophobic anticancer agents such as DOX<sup>37</sup> and PTX.<sup>38</sup>

In vitro anticancer effects of DOX/B20 and PTX/B20 against the KB cell line were then compared to those of free DOX and PTX, respectively (Figure 4). Drug/B20 exhibited higher cytotoxicity than the corresponding free drug. The IC<sub>50</sub> values of DOX/B20 and free DOX were 0.0357 and 0.1125  $\mu\text{g/mL}$ , respectively. Similarly, the IC<sub>50</sub> values of PTX/B20 and PTX were 0.1506 and 0.8587  $\mu\text{g/mL}$ , respectively. This demonstrated that nanosized drug delivery systems could enhance the uptake and increase the cytotoxicity of poorly water-soluble anticancer drugs.<sup>39–41</sup> This approach could potentially have even more applicability in multidrug-resistant cancer therapy because the loading of anticancer drugs into nanoparticles could help overcome P-gp efflux, increasing the translocation of the drugs into cancer cells.<sup>33,35,36</sup> DOX would be released from micelles in the cytoplasm and then entered the nucleus successfully due to the A-B-A structure of PEG-PLA-PEG, which is similar to the structure of the cell membrane double layer.<sup>34,42</sup>

## In vivo studies

It is well known that nanoparticles with a size range of 50–200 nm can accumulate to high levels in tumor tissues due to the enhanced permeability and retention (EPR) effect.<sup>43,44</sup> To monitor the biodistribution of the nanosized B20 system, FITC was tagged to the surface of B20 micelles by replacing PEG-PLA-PEG (2 K-10 K-2 K) with FITC-PEG-PLA-PEG, with 10 wt% B20. After intravenous injection into tumor-bearing mice, most of the micelles were distributed to the liver, while a small portion of the micelles was accumulated in the tumor (Figure 5A). Interestingly, the micelles progressively accumulated in the tumor and high fluorescence intensity was clearly observed 24 hrs after injections, while the fluorescent intensity of the liver decreased gradually. Further, except a small proportion of the micelles that remained in the



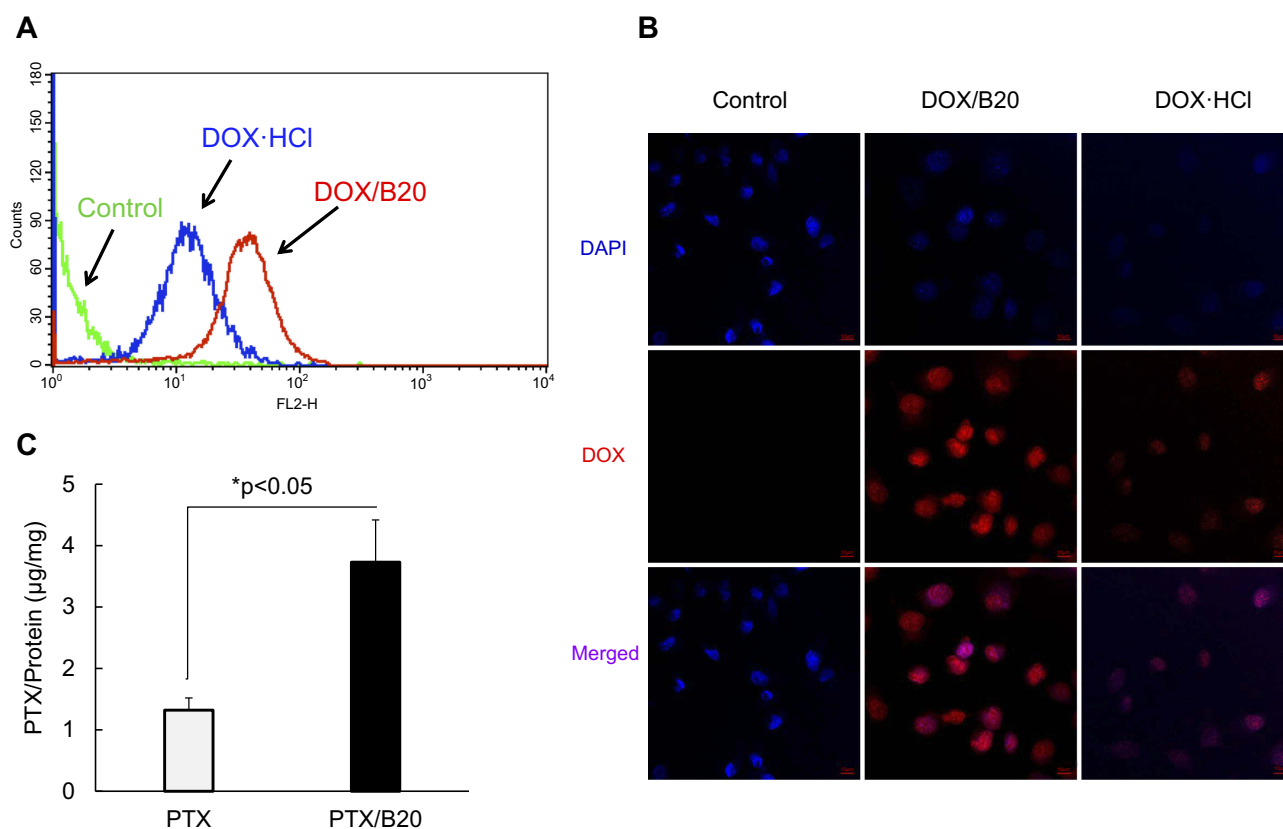


**Figure 3** Uptake of DOX/B20 into KB cells compared to that of DOX HCl determined using (A) flow cytometry and (B) confocal microscopy. (C) Uptake of PTX/B20 into KB cells compared to that of free PTX. A two-tailed Student's test was used to perform the statistical analysis.

**Abbreviations:** DOX, doxorubicin; PTX, paclitaxel.

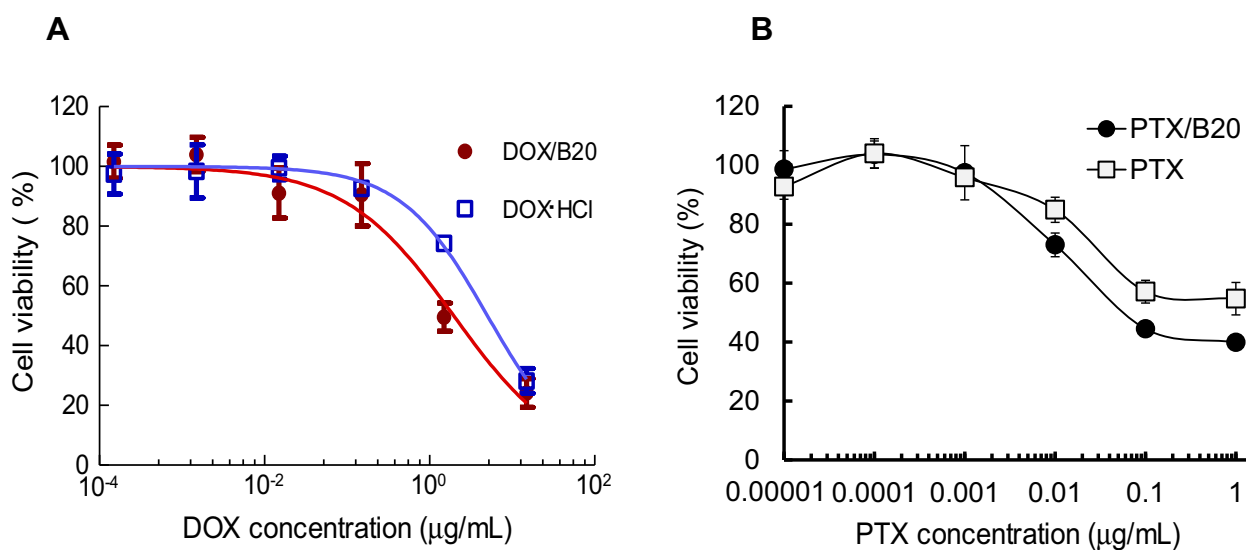


**Figure 4** In vitro anticancer effects of (A) DOX/B20 and (B) PTX/B20 against KB cells.

**Abbreviations:** DOX, doxorubicin; PTX, paclitaxel.

liver, little or no fluorescence signal due to the micelles was observed in other major organs 24 hrs after injection (Figures 5B and S3). This demonstrated that the blending system could result in selective accumulation in tumor

tissue. Interestingly, the accumulation of B20 in the spleen and liver was exceptionally low 24 hrs after injection, indicating very low clearance of the B20 micelles from circulation. This may have been due to their low CMC

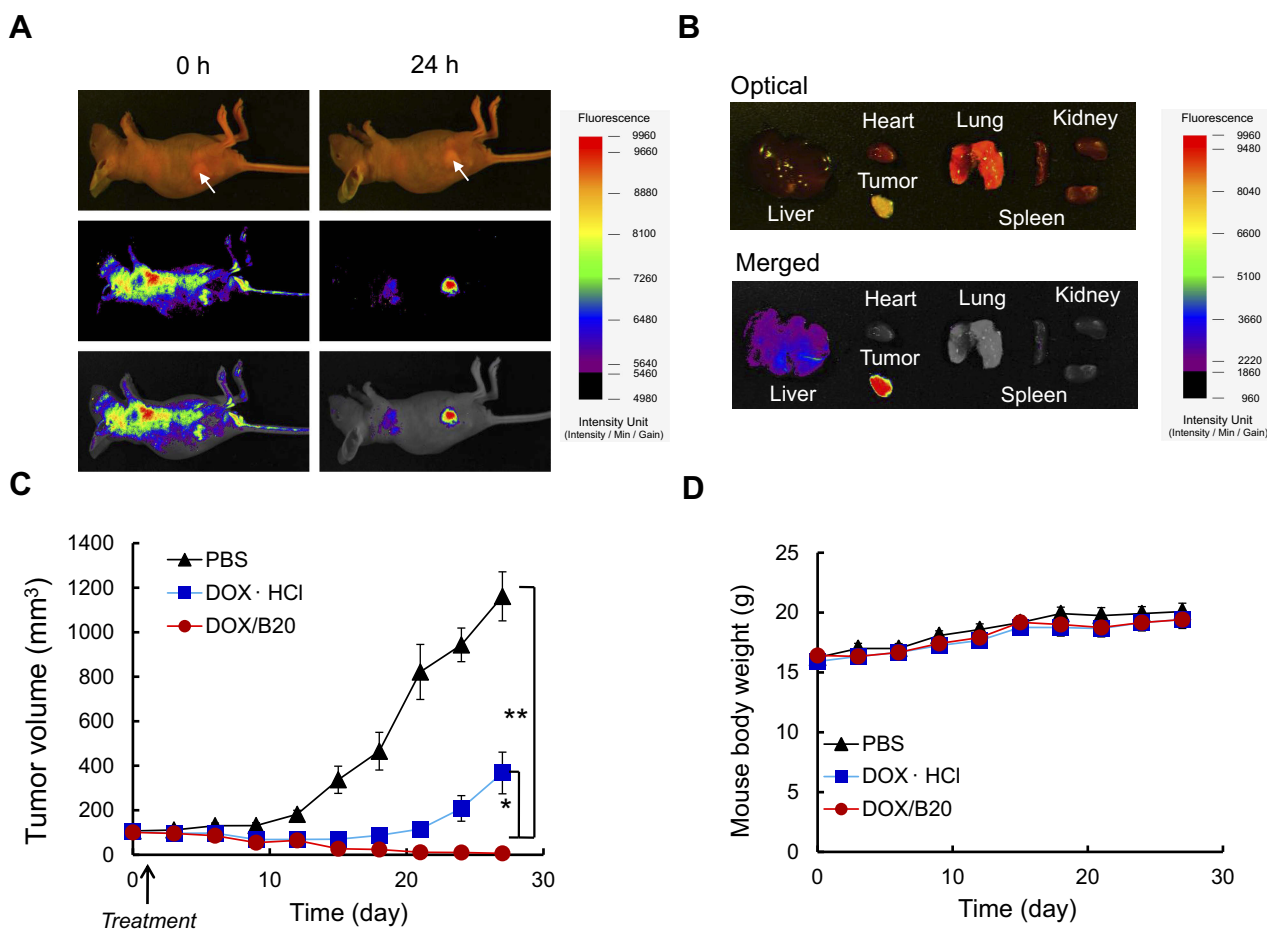


**Figure 5** In vivo studies. (A) Biodistribution of the nanosized micelles in tumor-bearing mice. Top, optical images; middle, fluorescent images; bottom, merged images. Arrows indicate tumors. (B) Accumulation of nanosized micelles in tumors and other organs 24 hrs after injection. Top, optical images; middle, fluorescent images; bottom, merged images. (C) Tumor volumes and (D) body weights of mice treated with DOX/B20, DOX HCl, or PBS. One-way ANOVA was performed. Dunnett's test was used for post hoc analysis. \* and \*\* indicate  $p < 0.05$  and  $p < 0.001$ , respectively. **Abbreviation:** DOX, doxorubicin.

and long-chain PEG (PEG 5 K) on their shells, which may have assisted the micelles in staying intact in the blood circulation and efficiently avoid attachment of the monophagocytic system in the liver and kidney.<sup>45–47</sup>

The in vivo anticancer efficacy of DOX/B20 was subsequently evaluated using KB tumor-bearing nude mice. It was found that a single i.v. administration of DOX/B20 caused clear tumor regression compared to DOX or saline administration; the saline-administered control group showed the most tumor growth with tumor volumes  $>1,000 \text{ mm}^3$  ( $n=6$ , mean  $\pm$  SEM, Figures 5C and S4). The superior anticancer effect of DOX/B20 compared to that of free DOX might have been due to tumor-targeted drug delivery because of the blending system. While free DOX was nonselectively distributed throughout the mouse body, DOX/B20 may have been highly and selectively accumulated in tumor tissues due to the EPR effect, resulting in the high concentration and long-lasting confinement of DOX at tumor sites. There were no significant

changes in body weights of mice in any of the three groups during the study period (Figure 5D); we surmise that a single drug dose showed no evident toxicity throughout the body. This further demonstrated that the blending system has high potential in the development of nanomedicines for cancer treatment.

## Conclusion

A blending system with high stability and high drug-loading capacity was prepared by combining PEG-PLA-PEG triblock copolymers of different molecular weights. The blending systems were prepared by combining 80 wt% of PEG-PLA-PEG triblock copolymer (2 K-10 K-2 K) and 20 wt% of PEG-PLA-PEG triblock copolymer (5 K-10 K-5 K). The system showed several advantages compared to a micellar system using a single type of triblock copolymer, in terms of colloidal stability and drug-loading capacity. Further, the drug-loaded blending systems showed significantly improved in

vitro anticancer effects and cellular uptake compared to those of free drugs. Corresponding to the results of the in vitro study, the drug-loaded blending system also showed more effective in vivo tumor growth suppression and accumulation in tumor tissue than free drug. From the perspective of pharmaceutical development, further toxicity and efficacy studies of PTX formulated with this system could advance its use in the development of anticancer drugs. Currently, efficacy and toxicity studies using PTX and the combination therapy of DOX and PTX for pharmaceutical application are in progress. The blending system reported here could be a potential nanoplat-form for poorly water-soluble drugs used in cancer treatment.

## Acknowledgments

This research was supported by a grant (16173MFDS542) from the Ministry of Food and Drug Safety in 2018 and by a National Research Foundation of Korea (NRF) grant funded by the Korean government (MSIP) (NRF-2014R-1A2A1A11050094 and 2015R1A5A1008958).

## Disclosure

The authors report no conflicts of interest in this work.

## References

- Shi J, Kantoff PW, Wooster R, Farokhzad OC. Cancer nanomedicine: progress, challenges and opportunities. *Nat Rev Cancer*. 2017;17(1):20–37. doi:10.1038/nrc.2016.108
- Wicki A, Witzigmann D, Balasubramanian V, Huwyler J. Nanomedicine in cancer therapy: challenges, opportunities, and clinical applications. *J Controlled Release*. 2015;200:138–157. doi:10.1016/j.jconrel.2014.12.030
- Peer D, Karp JM, Hong S, Farokhzad OC, Margalit R, Langer R. Nanocarriers as an emerging platform for cancer therapy. *Nat Nanotechnol*. 2007;2(12):751. doi:10.1038/nnano.2007.387
- Choi JY, Thapa RK, Yong CS, Kim JO. Nanoparticle-based combination drug delivery systems for synergistic cancer treatment. *J Pharm Invest*. 2016;46(4):325–339. doi:10.1007/s40005-016-0252-1
- Choi YH, Han H-K, JJoPI. Nanomedicines: current status and future perspectives in aspect of drug delivery and pharmacokinetics. *J Pharm Invest*. 2018;48(1):43–60. doi:10.1007/s40005-017-0370-4
- Allen C, Maysinger D, Eisenberg A. Nano-engineering block copolymer aggregates for drug delivery. *Colloids Surf B*. 1999;16(1–4):3–27. doi:10.1016/S0927-7765(99)00058-2
- Hoang NH, Lim C, Sim T, et al. Characterization of a triblock copolymer, poly (ethylene glycol)-polylactide-poly (ethylene glycol), with different structures for anticancer drug delivery applications. *Polym Bull*. 2017;74(5):1595–1609. doi:10.1007/s00289-016-1791-3
- Gong J, Chen M, Zheng Y, Wang S, Wang Y. Polymeric micelles drug delivery system in oncology. *J Controlled Release*. 2012;159(3):312–323. doi:10.1016/j.jconrel.2011.12.012
- Oh KT, Bronich TK, Kabanov AV. Micellar formulations for drug delivery based on mixtures of hydrophobic and hydrophilic Pluronic® block copolymers. *J Controlled Release*. 2004;94(2):411–422. doi:10.1016/j.jconrel.2003.10.018
- Lee ES, Oh YT, Youn YS, et al. Binary mixing of micelles using Pluronics for a nano-sized drug delivery system. *Colloids Surf B*. 2011;82(1):190–195. doi:10.1016/j.colsurfb.2010.08.033
- Pitto-Barry A, Barry NPJPC. Pluronic® block-copolymers in medicine: from chemical and biological versatility to rationalisation and clinical advances. *Nat Commun*. 2014;5(10):3291–3297. doi:10.1038/ncomms4291
- Food U. Drug administration %J -02-20. Inactive ingredient search for approved drug products; 2017. Available from: <https://www.accessdata.fda.gov/scripts/cder/iig/index.Cfm?event=browseByLetter.page&Letter=Pssdata.fda.gov/scripts/cder/iig/index.Cfm?event=browseByLetter.page&Letter=P>. Accessed March 22, 2019.
- Valle JW, Armstrong A, Newman C, et al. A phase 2 study of SP1049C, doxorubicin in P-glycoprotein-targeting pluronics, in patients with advanced adenocarcinoma of the esophagus and gastro-esophageal junction. *Invest New Drugs*. 2011;29(5):1029–1037. doi:10.1007/s10637-010-9399-1
- Lillevtedt M, Smistad G, Tønnesen H, Høgset A, Kristensen S. Solubilization of the novel anionic amphiphilic photosensitizer TPCS2a by nonionic Pluronic block copolymers. *Eur J Pharm Sci*. 2011;43(3):180–187. doi:10.1016/j.ejps.2011.04.004
- Magnusson G, Olsson T, Nyberg J-A. Toxicity of pluronic f-68. *Toxicol Lett*. 1986;30(3):203–207.
- Sim T, Kim JE, Hoang NH, et al. Development of a docetaxel micellar formulation using poly (ethylene glycol)-polylactide-poly (ethylene glycol)(PEG-PLA-PEG) with successful reconstitution for tumor targeted drug delivery. *Drug Delivery*. 2018;25(1):1362–1371.
- Song H-T, Hoang NH, Yun JM, et al. Development of a new tri-block copolymer with a functional end and its feasibility for treatment of metastatic breast cancer. *Colloids Surf B*. 2016;144:73–80. doi:10.1016/j.colsurfb.2016.04.002
- Hoang NH, Lim C, Sim T, et al. Characterization of a triblock copolymer, poly (ethylene glycol)-polylactide-poly (ethylene glycol), with different structures for anticancer drug delivery applications. *Polym Bull*. 2017;74(5):1595–1609.
- Hoang NH, Lim C, Sim T, Oh KT. Triblock copolymers for nano-sized drug delivery systems. *J Pharm Invest*. 2017;47(1):27–35. doi:10.1007/s40005-016-0291-7
- Lysenko EA, Bronich TK, Slonkina EV, Eisenberg A, Kabanov VA, Kabanov AV. Block ionomer complexes with polystyrene core-forming block in selective solvents of various polarities. 1. Solution behavior and self-assembly in aqueous media. *Macromolecules*. 2002;35(16):6351–6361. doi:10.1021/ma020048s
- Han SK, Na K, Bae YH. Sulfonamide based pH-sensitive polymeric micelles: physicochemical characteristics and pH-dependent aggregation. *Colloids Surf A*. 2003;214(1–3):49–59. doi:10.1016/S0927-7757(02)00389-8
- Duncan R. The dawning era of polymer therapeutics. *Nat Rev Drug Discov*. 2003;2(5):347–360. doi:10.1038/nrd1088
- Oh NM, Oh KT, Youn YS, Lee ES. Artificial nano-pin as a temporal molecular glue for the targeting of acidic tumor cells. *Polym Adv Technol*. 2014;25(8):842–850. doi:10.1002/pat.3315
- Oh NM, Oh KT, Youn YS, et al. Poly(L-aspartic acid) nanogels for lysosome-selective antitumor drug delivery. *Colloids Surf B*. 2013;101:298–306. doi:10.1016/j.colsurfb.2012.07.013
- Kwag DS, Oh KT, Lee ES. Facile synthesis of multilayered poly-saccharidic vesicles. *J Controlled Release*. 2014;187:83–90. doi:10.1016/j.jconrel.2014.05.032
- He C, Hu Y, Yin L, Tang C, Yin C. Effects of particle size and surface charge on cellular uptake and biodistribution of polymeric nanoparticles. *Biomaterials*. 2010;31(13):3657–3666. doi:10.1016/j.biomaterials.2010.01.065

27. Kwon GS, Okano T. Polymeric micelles as new drug carriers. *Adv Drug Del Rev.* 1996;21(2):107–116. doi:10.1016/S0169-409X(96)00401-2
28. Kim JH, Oh YT, Lee KS, Yun JM, Park BT, Oh KT. Development of a pH-Sensitive Polymer Using Poly (aspartic acid-graft-imidazole)-block-Poly (ethylene glycol) for acidic pH targeting systems. *Macromol Res.* 2011;19(5):453–460. doi:10.1007/s13233-011-0502-z
29. Lee ES, Kim JH, Sim T, et al. A feasibility study of a pH sensitive nanomedicine using doxorubicin loaded poly(aspartic acid-graft-imidazole)-block-poly(ethylene glycol) micelles. *J Mater Chem B.* 2014;2(9):1152–1159. doi:10.1039/c3tb21379j
30. Torchilin V. Targeted polymeric micelles for delivery of poorly soluble drugs. *Cell Mol Life Sci.* 2004;61(19–20):2549–2559. doi:10.1007/s00018-004-4153-5
31. Lee J, Cho EC, Cho K. Incorporation and release behavior of hydrophobic drug in functionalized poly (D, L-lactide)-block-poly (ethylene oxide) micelles. *J Controlled Release.* 2004;94(2):323–335. doi:10.1016/j.jconrel.2003.10.012
32. Verma A, Stellacci F. Effect of surface properties on nanoparticle–cell interactions. *Small.* 2010;6(1):12–21. doi:10.1002/sml.200901158
33. Ma P, Mumper RJ. Anthracycline nano-delivery systems to overcome multiple drug resistance: A comprehensive review. *Nano Today.* 2013;8(3):313–331. doi:10.1016/j.nantod.2013.04.006
34. Haag R. Supramolecular drug-delivery systems based on polymeric core–shell architectures. *Angew Chem Int Ed.* 2004;43(3):278–282. doi:10.1002/anie.200301694
35. De Verdiere AC, Dubernet C, Nemati F, Poupon M, Puisieux F, Couvreur P. Uptake of doxorubicin from loaded nanoparticles in multidrug-resistant leukemic murine cells. *Cancer Chemother Pharmacol.* 1994;33(6):504–508.
36. Wong HL, Bendayan R, Rauth AM, Xue HY, Babakhanian K, Wu XY. A mechanistic study of enhanced doxorubicin uptake and retention in multidrug resistant breast cancer cells using a polymer-lipid hybrid nanoparticle system. *J Pharmacol Exp Ther.* 2006;317(3):1372–1381. doi:10.1124/jpet.106.101154
37. Yang C, Sun Y, Zhang L. Dissipative particle dynamics study on aggregation of MPEG-PAE-PLA block polymer micelles loading doxorubicin. *Chin J Chem.* 2012;30(9):1980–1986. doi:10.1200/JCO.2011.39.2381
38. Huh KM, Lee SC, Cho YW, Lee J, Jeong JH, Park K. Hydrotropic polymer micelle system for delivery of paclitaxel. *J Controlled Release.* 2005;101(1–3):59–68. doi:10.1016/j.jconrel.2004.07.003
39. Zhu C, Jung S, Luo S, et al. Co-delivery of siRNA and paclitaxel into cancer cells by biodegradable cationic micelles based on PDMAEMA–PCL–PDMAEMA triblock copolymers. *Biomaterials.* 2010;31(8):2408–2416. doi:10.1016/j.biomaterials.2009.11.077
40. Kumar R, Kulkarni A, Nagesha DK, Sridhar S. In vitro evaluation of theranostic polymeric micelles for imaging and drug delivery in cancer. *Theranostics.* 2012;2(7):714–722. doi:10.7150/thno.3927
41. Melguizo C, Cabeza L, Prados J, et al. Enhanced antitumoral activity of doxorubicin against lung cancer cells using biodegradable poly (butylcyanoacrylate) nanoparticles. *Drug Des Devel Ther.* 2015;9:6433.
42. Feitosa E, Winnik F. Interaction between Pluronic F127 and dioctadecyldimethylammonium bromide (DODAB) vesicles studied by differential scanning calorimetry. *Langmuir.* 2010;26(23):17852–17857. doi:10.1021/la102603a
43. Maeda H, Wu J, Sawa T, Matsumura Y, Hori K. Tumor vascular permeability and the EPR effect in macromolecular therapeutics: a review. *J Controlled Release.* 2000;65(1):271–284.
44. Fang J, Nakamura H, Maeda H. The EPR effect: unique features of tumor blood vessels for drug delivery, factors involved, and limitations and augmentation of the effect. *Adv Drug Del Rev.* 2011;63(3):136–151. doi:10.1016/j.addr.2010.04.009
45. Zhang X, Burt HM, Mangold G, et al. Anti-tumor efficacy and biodistribution of intravenous polymeric micellar paclitaxel. *Anticancer Drugs.* 1997;8(7):696–701.
46. Huang S, Shao K, Kuang Y, et al. Tumor targeting and micro-environment-responsive nanoparticles for gene delivery. *Biomaterials.* 2013;34(21):5294–5302. doi:10.1016/j.biomaterials.2013.03.043
47. Kim SH, Lee JE, Sharker SM, Jeong JH, In I, Park SY. In vitro and in vivo tumor targeted photothermal cancer therapy using functionalized graphene nanoparticles. *Biomacromolecules.* 2015;16(11):3519–3529. doi:10.1021/acs.biomac.5b00944

## Supplementary material

### Methods

#### Characterizations of block copolymers

<sup>1</sup>H-NMR spectroscopy and gel permeation chromatography (GPC) were used to determine the MW and the composition of the block copolymers. <sup>1</sup>H-NMR was performed using Varian, Gemini 2000 (NMR 300 MHz) instrument (Varian, Palo Alto, CA, USA). CDCl<sub>3</sub> was used as solvent for analysis of block copolymers. The molecular weight of the PLA segment was determined from <sup>1</sup>H-NMR spectrum by examining the peak intensity ratio of the methine proton of the PLA segment (COCH(CH<sub>3</sub>)O: δ=5.2 ppm) and the methylene protons of the PEG segment (OCH<sub>2</sub>CH<sub>2</sub>: δ=3.6 ppm) based on the number-average molecular weight of PEG.<sup>1</sup> Number- and weight-average molecular weights (M<sub>n</sub> and M<sub>w</sub>, respectively) as well as polydispersity index (PDI=M<sub>w</sub>/M<sub>n</sub>) of the copolymers were determined by GPC using Agilent Technology series-1200 instrument, equipped with the refractive index detector. THF was used as the mobile phase at 1.0 mL/min of flow rate. Column temperature was set at 30°C. The copolymers were dissolved in THF, filtered, and injected into PLgel 10 μm MIXED-B column (Agilent). The molecular weight of block copolymers was calculated based on the calibration curve made from a series of polystyrene standards (Scientific Polymer Products Inc., Ontario, NY, USA).<sup>2</sup>

#### Doxorubicin release from micelles

For the DOX release test, 1 mL of DOX-loaded micelle solutions was transferred into dialysis membrane tubes (Spectra/Por<sup>®</sup>, MWCO 3.5 kDa). The dialysis membrane tubes were subsequently immersed in a vial containing 10 mL of PBS pH 7.4 and incubated in shaker water bath at a speed of 70 rpm and 37°C. At predetermined time points (1 hr, 3 hrs, 6 hrs, 9 hrs, 12 hrs, 24 hrs, and 48 hrs), the media in the vials were collected to determine the amount

of DOX released and the vials were replenished with 10 mL of fresh PBS pH 7.4. The amount of DOX released from the micelles was quantified by using UV-VIS spectrometer (GENESYS 10 UV, Thermo Scientific, Waltham, MA, USA) at wavelength λ=481 nm.

#### PTX release from micelles

For the PTX release test, 1 mL of PTX-loaded micelle solutions was transferred into dialysis membrane tubes (Spectra/Por<sup>®</sup>, MWCO 3.5 kDa). The dialysis membrane tubes were subsequently immersed in a vial containing 10 mL of PBS pH 7.4 and incubated in shaker water bath at a speed of 70 rpm and 37°C. At predetermined time points (1 hr, 3 hrs, 6 hrs, 9 hrs, 12 hrs, 24 hrs, 48 hrs, and 72 hrs), the media in the vials were collected to determine the amount of PTX released and the vials were replenished with 10 mL of fresh PBS pH 7.4. The collected PTX solutions were then lyophilized, and the amount of PTX released from the micelles was quantified by liquid chromatography (Agilent) with a UV detector at the wavelength of 230 nm.

## Results and discussion

### Characterization of PEG-PLA-PEG

PEG-PLA-PEG (5K-10K-5K) triblock copolymer and functional PEG-PLA-PEG (2K-10K-2K) were synthesized with the methods as reported.<sup>3-5</sup> The success of triblock copolymer synthesis was confirmed by <sup>1</sup>H NMR and GPC (Table S1, Figure S1). The peak at 3.6 ppm was assigned to proton **b** of PEG. The peaks at 5.2 ppm and 1.6 ppm were assigned to protons **a** and **c** of PLA, respectively. According to GPC analysis, the MW of PLA in two types of triblock copolymers were similar with the values in the range of 9–11 KDa. Since the two block copolymers had a similar length of PLA and a big difference in MW of PEG, they would probably possess different physicochemical characterizations, resulting in the unique properties of micelles.

**Table S1** Characterizations of triblock copolymers

PEG-PLA-PEG triblock copolymer	M <sub>n</sub>		PDI <sup>b</sup>	Code
	<sup>1</sup> H NMR	GPC <sup>a</sup>		
Functional 2 K-10 K-2 K	13,900	14,500	1.36	T2
5 K-10 K-5 K	24,600	19,100	1.23	T5

**Notes:** M<sub>n</sub>, Number-average molecular weight. <sup>a</sup>Based on polystyrene standards. <sup>b</sup>Polydispersity index (calculated from GPC data).

**Abbreviations:** PEG-PLA-PEG, poly(ethylene glycol)-poly(lactic acid)-poly(ethylene glycol); GPC, gel permeation chromatography; PDI, polydispersity index.



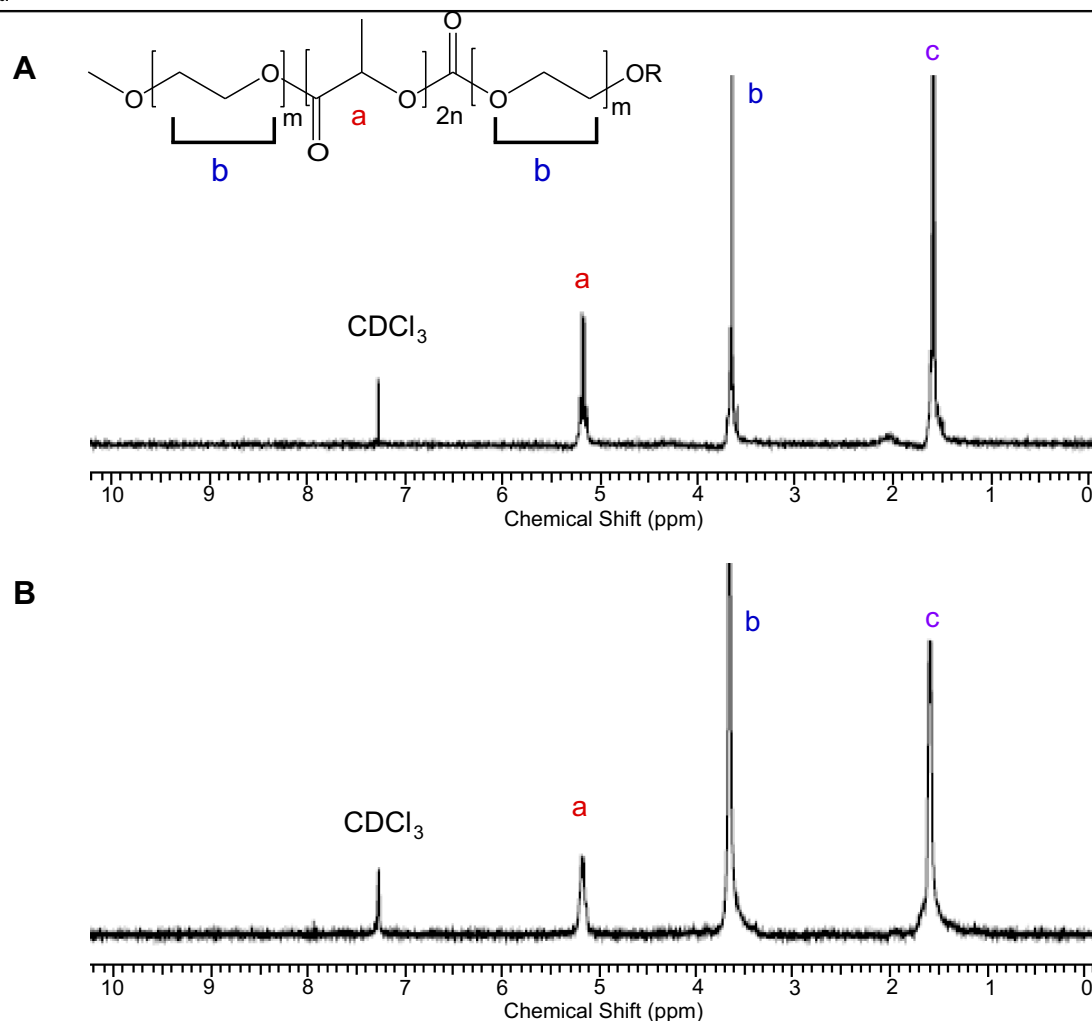


**Figure S1**  $^1\text{H}$  NMR spectrum of (A) PEG-PLA-PEG (2K-10K-2K, R=-CH<sub>3</sub>) and (B) functional PEG-PLA-PEG (5K-10K-5K, R=-H). CDCl<sub>3</sub> was used as solvent. **Abbreviation:** PEG-PLA-PEG, poly(ethylene glycol)-poly(lactic acid)-poly(ethylene glycol)

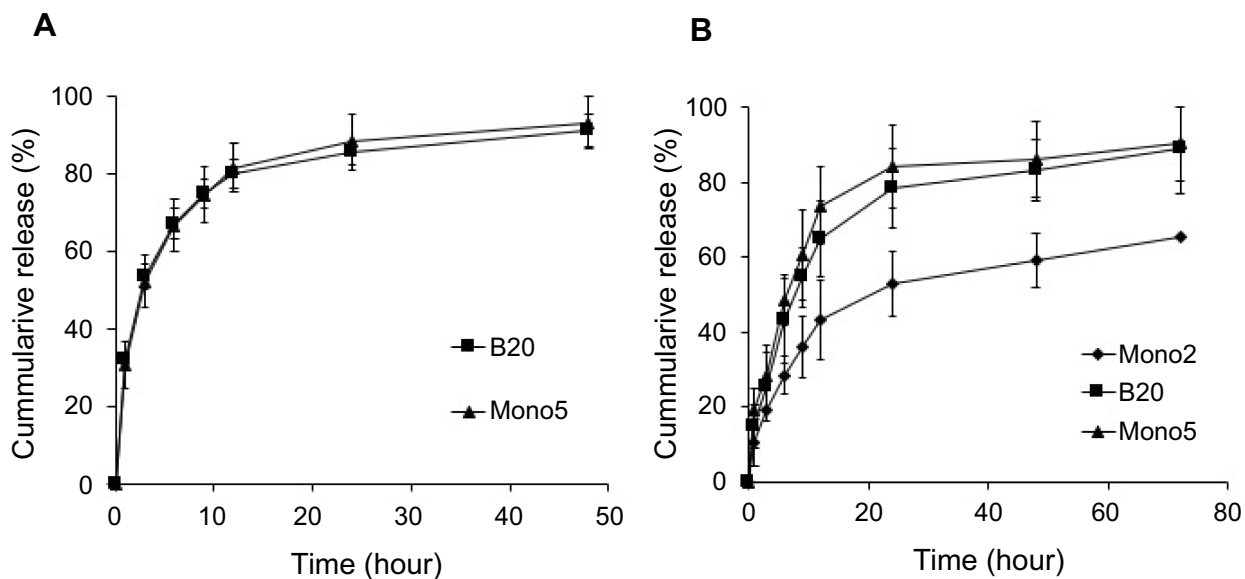


**Figure S2** Drug-release profile of blending system (B20) and original micelles (mono 2 and mono 5). (A) DOX release and (B) PTX release. For information on DOX release from Mono 2 see Hoang et al.<sup>6</sup> **Abbreviations:** DOX, doxorubicin; PTX, paclitaxel.

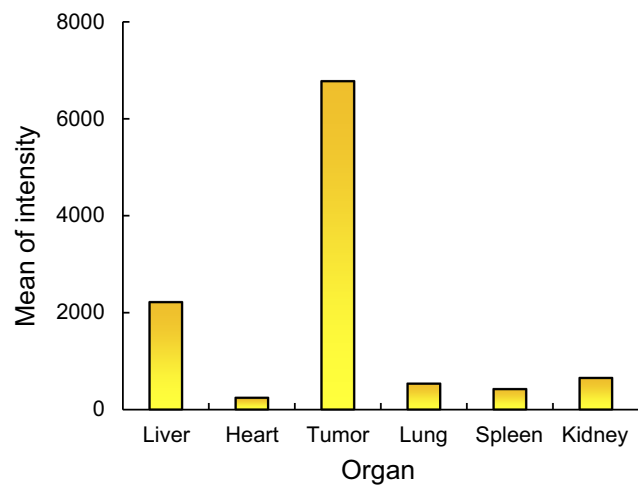


**Figure S3** Quantitative fluorescence intensities of tumor compared to those of different organs after 24 hrs from i.v. injection of the micelles.

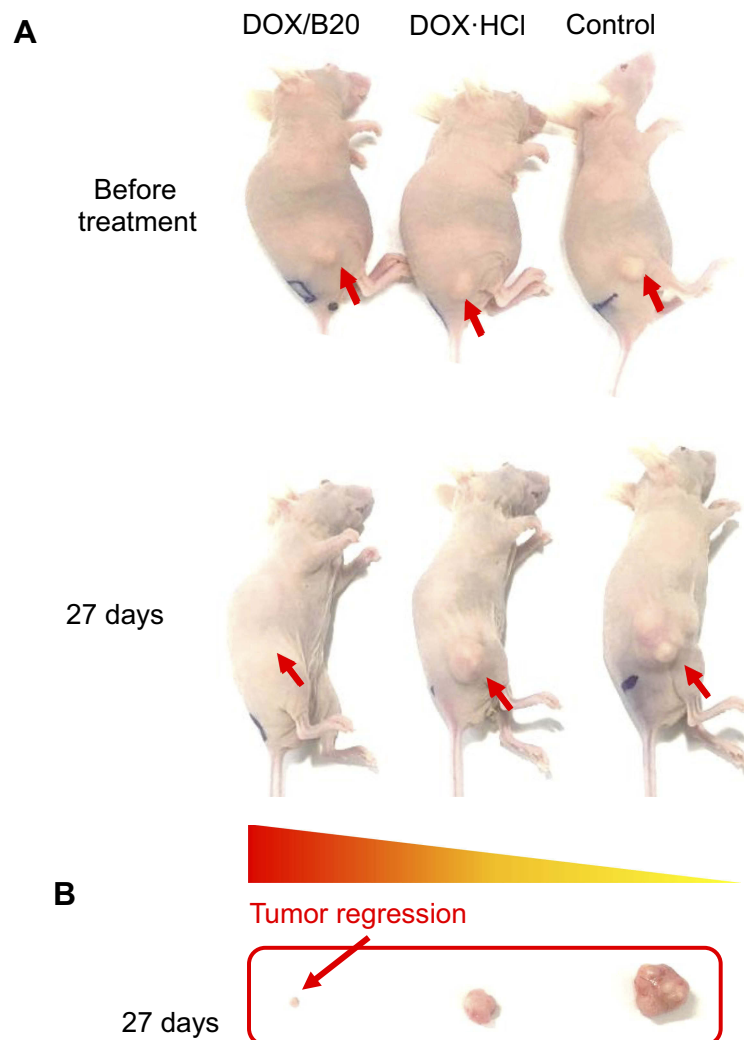


**Figure S4** In vivo tumor regression: (A) Balb/c nu mice 27 days after treatment. Arrows: tumors. (B) Extracted tumors in mice 27 days after treatment.

## References

1. Yasugi K, Nagasaki Y, Kato M, Kataoka K. Preparation and characterization of polymer micelles from poly (ethylene glycol)-poly (D, L-lactide) block copolymers as potential drug carrier. *J Controlled Release*. 1999;62(1):89–100.
2. Jain AK, Goyal AK, Mishra N, Vaidya B, Mangal S, Vyas SP. PEG–PLA–PEG block copolymeric nanoparticles for oral immunization against hepatitis B. *Int J Pharm*. 2010;387(1):253–262.
3. Oh KT, Yun JM, inventors; Chung-Ang University Industry-Academy Cooperation Foundation, assignee. BAB-type tri-block copolymer comprising polylactic acid (A) and polyethylene glycol (B), method for producing same, and drug delivery system using same. US patent US 9125944 B22015.
4. Hoang NH, Lim C, Sim T, et al. Characterization of a triblock copolymer, poly (ethylene glycol)-polylactide-poly (ethylene glycol), with different structures for anticancer drug delivery applications. *Polym Bull*. 2016;1–15.
5. Song H-T, Hoang NH, Yun JM, et al. Development of a new triblock copolymer with a functional end and its feasibility for treatment of metastatic breast cancer. *Colloids Surf B*. 2016;144:73–80.
6. Hoang NH, Lim C, Sim T, et al. Characterization of a triblock copolymer, poly (ethylene glycol)-polylactide-poly (ethylene glycol), with different structures for anticancer drug delivery applications. *Polym Bull*. 2017;74(5):1595–1609.

International Journal of Nanomedicine

Dovepress

### Publish your work in this journal

The International Journal of Nanomedicine is an international, peer-reviewed journal focusing on the application of nanotechnology in diagnostics, therapeutics, and drug delivery systems throughout the biomedical field. This journal is indexed on PubMed Central, MedLine, CAS, SciSearch®, Current Contents®/Clinical Medicine,

Journal Citation Reports/Science Edition, EMBase, Scopus and the Elsevier Bibliographic databases. The manuscript management system is completely online and includes a very quick and fair peer-review system, which is all easy to use. Visit <http://www.dovepress.com/testimonials.php> to read real quotes from published authors.

Submit your manuscript here: <https://www.dovepress.com/international-journal-of-nanomedicine-journal>